Transient aerodynamic pressures and forces on trackside and overhead structures due to passing trains. Part 1 Model scale experiments Part 2 Standards applications

Baker, Christopher; Jordan, S.; Gilbert, T.; Quinn, A.; Sterling, M.; Johnson, T.; Lane, J.

DOI:
10.1177/0954409712464859

Document Version
Early version, also known as pre-print

Citation for published version (Harvard):
Baker, C, Jordan, S, Gilbert, T, Quinn, A, Sterling, M, Johnson, T & Lane, J 2014, 'Transient aerodynamic pressures and forces on trackside and overhead structures due to passing trains. Part 1 Model scale experiments Part 2 Standards applications', *Proceedings of the Institution of Mechanical Engineers Part F Journal of Rail and Rapid Transit*, vol. 228, no. 4, pp. 36-69. https://doi.org/10.1177/0954409712464859

Transient aerodynamic pressures and forces on trackside and overhead structures due to passing trains. Part 1 Model scale experiments

C Baker*, S Jordan, T Gilbert, A Quinn, M Sterling

Birmingham Centre for Railway Research and Education, University of Birmingham, Birmingham B15 2TT

T Johnson, J Lane

RSSB, Block 2, Angel Square, 1 Torrens Street, London, EC1V 1NY

*Corresponding author – c.j.baker@bham.ac.uk, +44 (0)121 414 5067

Abstract

This is the first part of a two part paper that describes the results of an experimental investigation to measure the aerodynamic pressure forces on structures in the vicinity of railway tracks. The investigations were carried out in order to obtain a fundamental understanding of the nature of the phenomenon and to obtain data for a variety of railway infrastructure geometries of particular relevance to the GB situation, in order to provide material for a National Annex to the relevant Eurocode. The experiments were carried out on the moving model TRAIN Rig, with models of three different sorts of trains with different nose types, and a variety of infrastructures types – vertical hoardings, overbridges, station canopies and trestle platforms. The transient loads that were measured had a characteristic form – a positive pressure peak followed by a negative pressure peak. In general the magnitudes of the two peaks were different, and varied with infrastructure type and position, as well as with train type. As would be expected, the more streamlined the train, the lower were the magnitudes of the pressure transients. A comparison of the experimental results was made with a variety of existing model scale and full scale data and a broad consistency was demonstrated, within the limits that the rather different experimental conditions in the various cases would allow. An analysis of the scaling of these pressure transients was carried out, and it was shown that whilst there was a reasonable collapse around a theoretical formulation, the complexity of the flows involved meant that a general scaling formulation could not be achieved. Part 2 of this paper will consider the application of the results to the development of revised standards formulations.

Keywords – train aerodynamics, aerodynamic pressures, bridges, hoardings, canopies, platforms

1. Introduction

It is well known that passing trains generate unsteady transient aerodynamic pressures. This is illustrated in figure 1 (taken from [1]). Essentially as the train nose passes, the pressure rises rapidly above ambient pressure to a positive peak, then falls rapidly through ambient pressure to a negative (suction) peak, and then decays rather more slowly towards the ambient value. As the tail of the train passes, the process is reversed, with a negative peak followed by a positive peak. These pressure transients result in transient forces on trackside and overhead structures. The design requirements for these structures are contained in the Eurocode EN 1991-2:2003 'Traffic Loads on Bridges' [2]. The data on which this code is based were originally developed by the ERRI (European Railway Research Institute) D189 committee [3] and also forms the basis of a railway specific CEN (European Committee for Standardisation) standard [1]. The data are also used in the Technical Standards for Interoperability (TSI), which are being developed to allow trains to run across national boundaries within Europe. The infrastructure TSI [4] directs users to this document, whereas the rolling stock TSI [5] adopts rather different procedures for ensuring acceptable transient pressures from new trains, through the specification of transient pressure at specific points relative to the track.

This paper reports a series of experiments that were carried out to investigate the nose pressure pulses of trains and their effect on trackside structures, using moving model train experiments. This investigation had two broad aims. The first was to investigate the fundamental nature of the transient pressure loading on trackside and overhead structures for a wide variety of structure shape and different types of train. Controlled model scale experiments allow a much greater number of tests to be carried out than was possible with the full scale experiments and panel method calculations reported in [3] and thus enables a greater physical insight of the phenomenon to be obtained. The second aim was more practical, and aimed generally at improving the Eurocode by providing reliable measurement data for a number of different types of train, that would supplement the earlier measurements and replace the data from the now obsolete panel method calculations. Also [2] was based on test data from operations with continental gauge rolling stock, which have significantly larger vehicle cross-sections than GB rolling stock. Since the aerodynamic pressure loads and the loadings imposed by slipstreams are dependent on the distance from the train side or roof, they are generally overstated when applied to the GB network. Thus there is a specific GB requirement for the

development of alternative design rules to those in [2], which can then be incorporated into a national annex to the code, and it is likely that such rules could result in significant economies for GB trackside and overhead structures. This work was thus funded by RSSB with support from the GB Aerodynamics Working Group.

The work described in this paper was carried out using the TRAIN Rig – a moving model aerodynamic facility in Derby, owned and operated by the University of Birmingham (http://www.birmingham.ac.uk/research/activity/railway/research/train-rig.aspx). 1/25th scale models of three train types were used, with the loads being measured on a variety of trackside structures. The technique of model testing is based on the well established techniques of dimensional analysis, which allow the results of properly conducted model tests to be related directly to full scale conditions. The experimental set up and data analysis techniques are set out in section 2 of this paper. Section 3 then describes the main experimental results, and these are compared as far as possible with the results of other investigations in section 4. The results are discussed in terms of the scaling of the pressure coefficient time histories, in section 5 and the basic conclusions that arise from these experiments are then set out in section 6. In a companion paper (Part 2), these results will be used to investigate the adequacy of the current design criteria and to develop new, GB specific, design curves.

2. Experimental methodology

2.1 The TRAIN Rig and experimental models

The TRAIN (Transient Railway Aerodynamics INvestigation) Rig is a highly versatile moving model rig that can be used for a wide variety of aerodynamic investigations (Figure 2). In broad terms, it consists of a 150m long track along which model vehicles can be propelled, in both directions, at speeds of up to 75m/s. For the work described in this report, the Rig was operated at a nominal model speed of 40m/s (which was repeatable to within $\pm 1 ms^{-1}$ for any one run). In the current situation it specifically allows transient static pressures to be measured on trackside structures. As will be seen below, by suitably non-dimensionalising the measured pressures with the model velocity, this data can be applied directly to full scale conditions.

Experiments were carried out at a model scale of 1/25th for both the train and structure models. Three model trains were used in the experiments:

- The leading car and half a trailing car of the Class 390.
- A two car Class 158 multiple unit.
- A Class 66 locomotive.

These three vehicles represent the leading vehicles of a streamlined passenger train, a non-streamlined passenger train and an aerodynamically rough freight train respectively. Photographs of the 1/25th scale models are shown in Figure 3.

A number of different structure models, also at 1/25th scale, were also tested. These are described below, using the co-ordinate system illustrated in figure 4. This has an origin at the top of rail level at the centre of the track with *x, y* and *z* being the along track, across track and vertical distances respectively. On some occasions it is convenient to use the edge of the platform as the origin, and the co-ordinates from this point are *y'* and *z'*. The positions of the structures are defined by *Y* and *Y'* laterally from the track centre and the platform edge respectively, and by *h* vertically from the top of rail. The structures tested were as follows.

- 2m high hoardings, with return corners placed at the trackside and on platforms, at *Y*= 1.45m, 1.95m and 2.75m (0.7m, 1.2m and 2.0m from the nearest rail) and *Y'* = 0.2m, 0.7m and 1.2m from the platform edge. Pressures were measured at the centre line of the hoarding, 0.25, 0.75, 1.25 and 1.75m from the baase.
- Overbridges of different widths and heights mounted symmetrically above the track – specifically 10m wide overbridges, with height above the track *h*= 4.5m, 5.0m, 5.5m and 6.0m to represent the wide structure condition implicit within [2], and *h*= 4.5m high overbridges 10.0m, 6.0m, 3.0m and 1.5m wide to permit consideration of pressure variability with width. Pressures were measured 0.5, 1.5, 2.5 and 3.5m either side of the bridge centreline for the two wider bridges, and 0.38, 1.13, 1.88 and 2.63m from the bridge centreline for the two narrower bridges.
- Platform canopies of different heights with different back wall positions. The modelled heights above the track were *h* = 4.0m, 4.7m, 5.4m and 6.0m and the modelled back wall distances Y = 3.45m, 3.85m, 4.25m and 4.75m (2.7m, 3.1m, 3.5m and 4.0m from the nearest rail) - 16

configurations in total to permit consideration of typical GB canopy structures. Pressures were measured 0.21, 0.62, 1.04, 1.45, 1.87, 2.28, 2.70 and 3.11m from the edge of the canopy nearest the track.

- A trestle platform to represent newer GB platform structures, an increasing number of which are of lightweight construction. Pressures were measured 0.19, 0.56, 0.94, 1.31, 1.69, 2.06, 2.44 and 2.81m from the edge of the platform nearest the track.

Photographs of the 1/25th scale models are shown in figures 5. Full details of both the train and the structure models can be found in [6].

The model speed of 40m/s and scale of 1/25th resulted in a Reynolds number based on model height of 3.2 x 10^5, above the value of 2.5 x 10^5 specified in [1]. Preliminary tests were carried out on the overbridge structure (see below) at lower vehicle speeds of 20m/s and 30m/s , and no noticeable changes in the results were found when they were plotted in a dimensionless form.

2.2 Instrumentation

The model speed was measured using pairs of opposing photoelectric position finders and reflectors separated by 10m along the TRAIN Rig track. A bespoke interface unit automatically calculated the average speed of the train through the 10m test area based on the time taken for each of the beams to be broken. The approximate vehicle speed was predetermined from the tension in the firing cable, and a nominal value of 7.6-7.8kN was used for each run. This resulted in a vehicle speed of 40m/s ± 1m/s. Generally for each of the cases listed in the last section, two or three repeat runs were carried out.

The static pressure was measured using a total of 16 Sensor Technics HCLA12X5PB differential amplified pressure transducers, connected to a Measurement Computing LGR5325 A/D converter and data logger. Transducers with a ±1250Pa range were selected to avoid pressure signal clipping. The drawback was that a lower signal-to-noise ratio resulted for the structures furthest from the train. However the noise, position offset and other characteristics were acceptable for the required accuracy and were accounted for in post-processing and error analysis over a range of pressures. The transducers provided a linear frequency response up to a ceiling of 2kHz, above which no higher

physical frequencies were captured. This meets the requirements of [1] for moving-model pressure measurements at this scale and speed. The sampling rate was significantly higher and linear smoothing was applied in post-processing (described in Section 3.1).

For the runs with the overbridge models, the hoarding models and the trestle platform model, the transducers were connected between the surface pressure tappings and a reference pressure measurement position beneath the TRAIN Rig track i.e. the pressure variation on the surface of the structure next to the track / train was measured. For the canopy models however the differential pressure between the top and bottom of the model was measured. For the overbridge, hoarding, and trestle tests the transducers were flush-mounted in the tappings, whilst for the canopy tests the transducers were connected remotely via 34mm long silicone tubes with internal diameters of 1.8mm.

For all the data that is presented below, the results are plotted in conventional pressure coefficient form defined as

$$C_p = \frac{p}{0.5\rho V^2} \quad (1)$$

where p is the measured pressure (relative to ambient), ρ is the density of air and V is the train velocity. This format effectively removes the effect of small variations in velocity from the pressure measurements, and the theory of dimensional analysis then allows these results to be applied to the full scale situation (assuming scale - Reynolds' number - effects are small). The pressure coefficient variation is described in terms of a distance relative to a fixed point at the trackside, expressed in full scale values. This procedure removes the effects of small scale velocity changes on the time scale and makes the results immediately applicable to the full scale situation. The figures that follow thus show the pressure coefficient distribution with reference to a fixed position on the train, the pressure coefficient effectively moving with the train.

We thus have two prime experimental variables – the pressure coefficient, and the distance relative to the train. A proper appreciation of the results that follow requires an indication in the uncertainty of these parameters. We consider first the pressure coefficient. From the above definition, the three physical parameters that are used in the calculation are pressure, vehicle speed and density. Now a

calibration of the pressure transducers shows that, for pressure differences of around 1000Pa (which will be seen is in the region of the maximum pressure that was measured), the standard error was 0.6%. For the velocity, taking into account the uncertainty in the distance between the photoelectric beam detectors and their response, a standard error of around 0.2% was calculated. Taking into account the variability of atmospheric pressure and temperature, the standard error on the density was found to be 1%. Thus the standard error on a pressure coefficient of 1.0 was (0.6% + 2*0.2% +1%) = 2%. This is a standard error of 0.02 on pressure coefficient throughout the range of the pressure coefficient. For the distance the uncertainty was effectively 25 x velocity x (1/sampling rate), which for a velocity of 40m/s and a sampling rate of 6250 samples / sec gives an uncertainty of 0.16m in terms of full scale values, which is small in relation to the length of a typical vehicle (25m).

3. Major experimental results

3.1 Repeats and smoothing of data

Figure 6a shows the raw data for three runs using the Class 390 running under the 10m wide, 4.5m high overbridge for the track centreline pressures (y=0m). The results are plotted in pressure coefficient form and the horizontal axis is given in terms of a distance, rather than a time, and thus effectively gives the shape of the pressure distribution relative to the train position, with negative x values roughly corresponding to distances ahead of the train nose. The zero distance position in the x direction is located at the point where the pressure transient passes through zero between the maximum and minimum peaks. This point corresponds approximately to a position on the train near where the full body cross-sectional area is immediately adjacent to the point on the structure where pressures are being measured. The pressure coefficients show an initial rise to a high positive peak followed by a rapid fall through zero to a negative, i.e. suction, peak, before a gradual return to a zero value through a series of small oscillations. It will be seen that this pattern is repeated in most of the datasets that follow, and is consistent with that measured by other investigators – see figure 1 for example. Two further points are apparent. Firstly there is very little difference between the three sets of results plotted in this way, and that secondly a high frequency oscillation can be seen on all the traces. It is thought that the latter is due to the structure model vibration caused by the passing train. Figure 6b shows the pressure coefficient data for hoardings but smoothed with a 10 point moving average filter. The high frequency oscillation has been eliminated. A number of other more complex

filtering methods were investigated, but proved to have little advantage over the simple moving average methodology. There was very little variation between runs for almost all the data that was obtained. The exception was for some runs using the Class 66 locomotive, where there were considerable fluctuations for large positive values of distance, after the passage of the train nose, presumably due to turbulence in the wake of the train. Such distances however do not correspond to regions of critical (maximum) pressure coefficients, which are known to occur around the train nose. Thus in what follows we will present data from individual runs only, although in each case multiple runs were carried out to check basic repeatability, and a 10 point moving average filter will be applied to all data.

3.2 Hoarding results

Figure 7 shows summary details for all three types of train at a height of z (above top of rail) or z' (above the platform surface) = 0.25m from the bottom of the hoarding. The results at this height are similar, if not somewhat greater than, those at other heights. The positive and negative peaks occur as would be expected, although for the trackside hoardings the negative peak is somewhat less obvious than for the platform cases, but note the two situations are not strictly comparable. The magnitudes of the coefficients decrease with distance from the nearest rail or platform edge. In general, the magnitudes of the Class 66 pressure coefficients are higher than for the Class 158 coefficients, which are themselves higher than for the Class 390 coefficients. In Figure 8, the coefficients are plotted for the hoarding positions closest to the track or the platform edge for all trains. Again these plots show the differences in the nature of the suction peaks between the trackside and platform cases, and the relative magnitudes of the peaks for the different train types can be appreciated. It is apparent from the figures that the forms of the positive pressure peaks are very smooth and consistent, but the negative pressure peak forms are less consistent, particularly for the blunt fronted Class 158 and Class 66. In some cases a double negative peak is apparent. It is surmised that this is due to an interaction between the pressure transient and what will be a significant separation region around the nose of these vehicles.

3.3 Overbridge results

Figure 9a shows a lateral plot of peak to peak pressure coefficients for the Class 390 passing beneath 10m wide overbridges at different heights, for different distances from the centre line of the overbridge. The results are broadly symmetrical about the centre line of the bridge. The scale of the pressure transient and the flow of the nose around the vehicle are similar to the scale of the overbridge, and complex interactions might be expected to occur between the flow and the structure. Note that the pressures furthest from the centre line are effectively between the bridge legs. Figure 9b shows a comparison between the centre line pressure coefficients for the different overbridge heights (the average of the coefficients measured at the tappings on either side of the centre line), and it can be seen that there is a consistent drop in pressure coefficient magnitudes as the height increases. Figures 9c and 9d show similar figures for the Class 390 beneath 4.5m high overbridges of different widths. The effect of varying width can be seen to be small in Figure 9d, except for the smallest overbridge width of 1.5m where the positive and negative peaks are significantly reduced. This is perhaps surprising as one might have expected an increase in load as the overall loading on the overbridge will be more coherent for a smaller structure. The possible interaction between the overbridge and the unsteady flow field, mentioned above, may however also be significant in this case. Similar data is shown for the Class 158 in Figure 10 and for the Class 66 in Figure 11. In general the magnitudes of the coefficients for the Class 158 are higher than for the Class 390, and the magnitudes for the Class 66 are higher still. The same comments apply as for the Class 390, although for the smaller overbridge widths for the Class 66, the suction peak close to x=0m, is small and dominated by a larger, unsteady peak someway downstream, which may be caused by pressure changes in the train boundary layer (slipstream). The differences between vehicles are illustrated in Figure 12 for centre line pressures for the 4.5m high, 10m wide overbridge. Note that the pressure gradient between the maximum and minimum peaks is higher for the Class 66 than for the other trains (or alternatively the peaks are closer together). This reflects the blunter nose shape of the Class 66.

3.4 Canopy results

The results of figure 13 show how the pressure coefficients vary away from the track across the canopy for the smallest back wall distance (2.7m from the nearest rail) and the lowest canopy height (h=4m), for all three train models. Essentially they show the expected shape of the other results, and

although the value for the tappings nearest to the canopy edge is always higher than the other tappings, there is actually relatively little variation in coefficient across the canopy for each train type. The Class 390 results have the smallest coefficients, and the Class 66 results have the highest. One significant feature, apparent on both the Class 158 and Class 66 results are the existence of pressure coefficient oscillations of a substantial magnitude downstream of the initial maximum and minimum peaks. A simple dynamic vibration test showed that this was not due to structural oscillations. It could thus be surmised that this is due to a vertical flow oscillation between the platform and the canopy, but more work would be required to substantiate this. A further interesting point is that the pressure coefficients near the edge of the canopy, although being higher than the other pressure coefficients, tend to lag the others to some extent, suggesting a distorted pressure wave within the canopy space. Figure 14 shows summary results for all three trains for the smallest and largest canopy heights, and the smallest and largest back wall distances, for the pressure tappings nearest the edge of the canopy. The results for the intermediate canopy heights and the intermediate back wall distances all fall consistently between these extremes. Again the Class 390 values are the smallest and the Class 66 values the largest. The peak magnitudes for the lowest canopies are significantly higher than for the highest as seems sensible. The oscillations in the wake can again be clearly seen. There is a suggestion that, for the Class 390 and Class 66, the frequency of the oscillation is related to canopy height, but this is not the case for the Class 158, where the frequencies look the same. This suggests that the oscillation frequency is not a simple function of structure dimensions. Figure 15 shows the effect of different back wall distances on the pressures at the edge of the canopy, for the Class 66 model, with a 4.7m high canopy. The no back wall results are also shown. It can be seen that the back wall distance, and indeed the presence or otherwise of the back wall, has only a limited effect on the measured pressures at this measurement position. This is generally true for all measurement positions. The no back wall results show a reduction in the positive pressure peak, but are otherwise very similar to those with a back wall. It is of interest to note that the pressure coefficient oscillations still exist for the open canopy, which suggests that they are due to vertical standing wave patterns in the cavity. Finally, Figure 16 shows a comparison for the pressure coefficients at the canopy edge for the lowest canopy, smallest back wall distance and for all three trains. This clearly shows the relative magnitudes of the pressure coefficient due to different train types (maximum for Class 66 and minimum for Class 390), including the downstream oscillations.

3.5 Trestle platform results

In general, as might be expected, for the trestle platform the magnitudes of the coefficients decrease with distance from the edge of the platform. A comparison of the pressure coefficients for the different vehicles, for the pressure tapping nearest the edge of the platform, is shown in Figure 17. Again the high pressure and suction peaks can be seen, although the Class 66 suction peak is less distinct than for the other vehicles. As before the Class 66 produces the highest positive and negative magnitudes of pressure coefficient.

4. Validation / comparison with other sources of data

This section discusses the validation of the current experimental results and presents a comparison with experimental data from other sources, in order to show that the results are reliable and can be used with confidence to predict full scale pressure distributions. In this process a number of different approaches are possible.

- Consideration of the internal consistency of results
- Consideration of earlier comparisons made with experimental results in the TRANSAERO Project, [7]
- Comparison with earlier TRAIN Rig measurements, [8]
- Comparison with full scale UK measurements on train sides, [8]
- Comparison with full scale UK measurements on platform hoardings, [9]
- Comparison with full scale UK measurements on a trestle platform, [10]

Internal consistency of results.

Firstly, it will be clear from the results discussed in section 3, that the data is internally consistent, in that it is of the same form in most cases, with the magnitudes of the coefficients being in general greatest for the Class 66 and least for the Class 390, with a consistent variation of magnitude with structure height / width, distance along and across the various structures. It is also quite repeatable on a run to run basis. This consistency and repeatability gives some confidence in the results.

TRANSAERO results

In the 1990s, as part of the EU TRANSAERO Project, measurements were made using the TRAIN Rig with moving models of Italian ETR500 trains, with various nose shapes, and the pressures measured on the side of stationary trains [7]. These results were compared with equivalent full scale measurements of the same configurations and excellent agreement with nose and tail passing pressures was obtained, again giving some confidence in the use of the rig for the measurement of train-induced pressures. For the full scale experiments the values of the maximum pressure peak, minimum pressure peak and time between the peaks were 0.222kPa, 0.253kPa and 0.122sec, whilst the equivalent values from the TRAIN Rig experiments were 0.220kPa, 0.241kPa and 0.112sec, indicating a high level of agreement.

Earlier TRAIN Rig measurements

Measurements have been made in the past using the TRAIN Rig on the pressures on stationary trains as they are passed by a moving train [8]. In this comparison three sets of such experimental data were used.

- A Class 341 multiple unit passing a Mark 3 coach, with pressures measured 1.63m above the track on the latter.
- A Class 43 (HST) passing a freight wagon, with the pressures being measured 1.63m and 2.73m above the track on the wagon.
- A Class 220 passing a freight wagon, with the pressures being measured 1.63m and 2.73m above the track on the wagon.

In calculating the equivalent hoarding distances, it was assumed that the width of the moving trains and the Mark 3 coach was given by the maximum width of the W6a gauge (2.82m) and the width of the freight container was 2.5m. This resulted in equivalent hoarding distances from the track centre line of 1.99m for the Class 341 / Mark 3 measurements and 2.31m for the other measurements. In view of the assumptions made above there could be potentially sizeable errors in these figures (of the order of ten centimetres or more). The average maximum and minimum pressure coefficients from between 3 and 6 sets of measurements in each case were calculated and these were compared with the height averaged values measured on the hoardings on the TRAIN Rig. The results of this comparison are given in Figure 18. The current TRAIN Rig data is shown as solid lines (connecting

the discrete experimental points), whilst the various sets of earlier data are shown as experimental points. “Max” refers to the maximum value of the positive pressure peak, and “Min” refers to the largest magnitude of the negative pressure peak. The full scale data is all for passenger train shapes with the leading vehicles all having relatively blunt noses. It can be seen that in general the present results are consistent with the earlier results, making due allowance for the variation in geometry, and the uncertainty in assigning the correct equivalent distance of a hoarding from the track centre line for the train side results. In general the maximum positive values correspond to the Class 390 and Class 158 data as would be expected, whereas the maximum negative values fall closest to the Class 158 data.

Full scale UK measurements on train sides

Full scale measurement data are also available for full scale experiments with a moving Class 390 train passing a stationary Class 390 train, with two measurement positions on the stationary train [8]. This can be compared with the hoarding data obtained for the Class 390, if equivalent distances from the track can be specified. The results are shown in Figure 19. It can be seen that, allowing for the differences in geometry between the two cases, the agreement is good, with close correspondence of the positive peaks, and the full scale negative peaks being rather greater in magnitude than the model scale values. This is probably due to differences in the track geometry in the full scale and model scale cases.

Full scale UK measurements on platform hoardings

Measurements were made at Northallerton of the pressures on a dummy wall on the station platform as it was passed by a variety of train types [9]. The trains were as follows

- Class 43 (HST) – one run
- Class 91 service train – two runs
- Class 91 test train – three runs
- A freight train with tankers - one run

The wall was 2m away from the platform edge and measured 14m in length and 3m in height. Measurements were made at heights of 0.095m, 1.33m and 2.04m above the platform. The average

peak to peak values of pressure coefficient for each type of train were averaged over the runs, and then the height averaged values of peak to peak coefficients for each train type were calculated. These were then compared with the height averaged values from the hoardings measured in the TRAIN rig. The results of the comparison are shown in Figure 20. The current TRAIN Rig data is again shown as solid lines and the full scale measurements as discrete symbols. Clearly the full scale tests were at a distance from the platform edge not covered by the model scale experiments, but the results are nonetheless consistent, with the passenger train full scale values being on plausible extrapolations of the Class 390 and Class 158 lines, and the freight train data being similarly consistent with the Class 66 data.

Full scale UK measurements on a trestle platform

Measurements were made of the pressures on the trestle platform at East Midlands Parkway Station [10]. Measurements were made of the absolute pressure on the upper surface of the platform at the platform edge and 1.5m from the edge, and differential pressure measurements were made between the upper and lower platform surfaces at the platform edge. Pressure measurements were made during the passage of Class 222 Meridian trains. There were data from 8 runs in total, and when the pressure coefficients were plotted against train speed little systematic variation could be seen. The pressure coefficient results were thus averaged across all runs, and the absolute pressure values compared with the equivalent absolute values from the TRAIN Rig experiments. The results of the comparison are shown in Figure 21. The full scale results for the streamlined Class 222 multiple unit compare well with the Class 390 data as might be expected.

5. Discussion

In this section we discuss the fundamental nature of the pressure transients measured in this report. We consider firstly how these pressure transients relate to the velocity field around the nose of the train, and thus to measurements of train slipstreams (see [11] for example). Secondly we consider if it is possible to parameterise the results in a relatively simply way, that might prove useful as a framework for applying these results to practical situations.

Firstly, it is clear that the pressure transients are well defined with a high level of repeatability from run to run, at least for the positive pressure part of the transient. This suggests that the transients are not affected by train induced turbulence and can effectively be described using inviscid potential flow considerations. This is to some extent confirmed by slipstream velocity measurements (see [12] for example) where the nose velocity peak is equally repeatable from run to run, in stark contrast to the flow in the train boundary layer and wake where there is very significant run to run variability caused by large scale turbulence flow structures. Now by a simple application of Bernoulli's equation it is possible to show that, in the inviscid flow field around the train nose, the pressure coefficient is given by

$$C_p = 1 - (1-u)^2 - v^2 - w^2 \qquad (2)$$

where *u, v* and *w* are the longitudinal, lateral and vertical slipstream velocities normalised with train velocity. *w* is always small (of the order of 0.02) and can be neglected. Typical velocity traces for *u* and *v* (from [11] for an ICE-1) are shown in figure 22. Note that there are small non-zero velocity values upstream of the train, caused by low level ambient wind flows. It can be seen that values of *u* and *v* of around 0.05 to 0.1 are measured. Such values enable one to write.

$$C_p \approx 2u \qquad (3)$$

From figure 22 it can be seen that the longitudinal velocity transient has a very similar form to the pressure transients measured here, giving some confidence in the above analysis. This suggests that pressure transients might be inferred from full scale velocity measurements, and vice versa. Equation (3) also implies that, as the pressure coefficient is proportional to longitudinal velocity, then if a vertical wall (or hoarding) is placed at this point then this can simply be represented by an "image" source on the other side of the wall, which would result in the following expression

$$C_p \approx 4u. \qquad (4)$$

Now the data from figure 22 corresponds to a position 0.5m above the top of the rail, 2.1m from the nearest rail, for a high speed train slipstream. The maximum pressure coefficient at a point 0.25m above the track, 2.0m from the nearest rail shown in figure 7 for the Class 390 (the nearest equivalent

to the full scale results, although rather more streamlined than the ICE-1) is around 0.17. From figure 22 and equation (4) the predicted value would be around 0.20, suggesting that the above argument is broadly valid.

Now let us consider the parameterisation of the experimental results. The basic questions are how and why the pressure transients vary with train type, distance from the train etc. We base our discussions around the two perhaps most fundamental cases of those studied – the trackside hoardings and the 10m wide overbridge i.e. vertical surfaces next to the track and horizontal surfaces above the track. We also use as a framework for the discussion the work of [13], which sets out a potential flow calculation of the forces on a vertical pedestrian barrier parallel to the track as a train passes by. Whilst the situation considered here is considerably more complex that that analysed by [12], it is felt that that analysis could act as a framework for the consideration of the parameterisation of the current results. That paper gives the following expression for the transient pressure force coefficient on a vertical structure next to the track.

$$C_F = \frac{3HA}{4Y^3}\frac{(x/Y)}{(1+(x/Y)^2)^{2.5}} \qquad (5)$$

Here *H* is the height of the barrier and *A* is the area of the train behind the nose. In terms of the current results, this suggest that the distance scales on the distance from the train centre *Y*, and that the pressure / force coefficients should scale on the cross sectional size of the train (presumably allowing for any large scale flow separation around the nose) and with Y^{-3}. This curve, plotted as $4C_F Y^2/3HA$ against x/Y is shown in figure 23. It can be seen to be of the expected form, and is anti-symmetric around the origin. Now clearly the experimental results shown in section 3 lack this degree of symmetry with the magnitudes of the positive and negative *x* pressure coefficient time histories being significantly different. We thus explore in what follows whether the traces for the negative and positive *x* portions of these curves scale in the way suggested by equation (5). To enable this comparison to be made the hoarding and overbridge data has been analysed to give overall forces in the *x* direction through either finding the height averaged pressure coefficient (for the vertical hoardings) or the pressure coefficient averaged over a 2m length at the centre of the overbridge span. These have then been aligned so that the zero crossing between the positive and negative peaks is at the origin in the *x* direction. Table 1 shows the maximum and minimum values for each case

considered together with the distances of these peaks from the origin. The ratio of the magnitudes of the maximum and minimum peaks and the ratio of the distances to the peaks are given, as an indication of the lack of symmetry. In addition, for each set of cases for any one train, the power law exponent for the variation of the maximum and minimum coefficients with respect to *Y* (for the hoarding) or bridge height *h*, and is given. Similarly the power law exponent for the variation of the position of the peaks with *Y* is also given. It can be seen from table 1 that there is a considerable degree of asymmetry, both in the maximum and minimum values and the positions of these values. Whilst some trends are apparent in the data, it is difficult to generalise. The slopes of the best fit lines with *Y* show that for the vertical hoardings, the peak values fall off with distance from the train with an exponent somewhere between 1 and 2 whilst for the overbridge case the exponent takes on values of 2.5 to 4.0 the latter being closer to the value of 3.0 expected from equation 5. Both the positions of the maximum and minimum peaks increase with distance from the train (i.e. the peaks become more spread out and diffuse), although the variation with *Y* or *h* has an exponent of rather greater than the value of unity that would be expected by the scaling with distance from the track centre line suggested above.

These points being made, the experimental data was then normalised with the magnitudes of the positive and negative peaks, and the magnitudes of the peak positions – effectively assuming different scaling for positive and negative values of *x*. The results are shown for the three classes of configuration in figure 24 and compared with the form of equation (5). It can be seen that the data fits this form well between the positive and negative peaks, but deviates significantly for regions outside the peaks. Inspection of the results shows that in general the greatest deviation is for small values of *Y* or *h*, i.e. with the structures close to the train.

Thus it can be concluded that the scaling of the pressure coefficient time histories is complex and not amenable to a general parameterisation, although the theoretical curves of [13] do give a useful framework for analysis and discussion.

6. Conclusions

From the data presented in the preceding sections the following main conclusions can be drawn.

a) The use of the TRAIN rig methodology has been shown to be a robust way of obtaining aerodynamic loading on a wide variety of trackside structures in an efficient manner, with the results showing good run-to-run repeatability.

b) The nose pressure coefficient distribution caused by passing trains is of the expected type, with a positive pressure peak followed by a negative pressure peak. In general, the peaks are not symmetrical i.e. they do not have the same magnitudes.

c) In general the surface pressure coefficients generated by the class 66 freight locomotive are greater than those generated by the class 158 multiple unit, which are themselves greater than those generated by the Class 390 Pendolino.

d) For the hoarding structures, the trackside negative peak is very indistinct.

e) The pressure coefficients across the overbridges, show a roughly parabolic fall off from the centre line. The coefficients fall as overbridge height increases, but are insensitive to the width of the bridge in the along track direction, except for the smallest bridge widths.

f) The canopy pressure coefficients show little variation across the canopy, except very close to the canopy edge. The effect of back wall distance on the canopy pressures is also small. For the blunter trains, a vertical standing pressure wave appears to be generated in the canopy / platform space.

g) A comparison of the current results with a range of earlier measurements and calculations at both model scale and full scale show a reasonable agreement, although the nature of many of the earlier results makes a precise comparison difficult.

h) There are indications that the surface pressures transients on vertical surfaces such as hoarding are well correlated with slipstream velocities.

i) The scaling of the pressure transient time histories is complex and not amenable to easy generalisation. That being said, the theoretical approach of Sanz-Andres et al (2004) offers a potentially useful framework for the consideration of these results.

References

[1] BSI Railway applications — Aerodynamics — Part 4: Requirements and test procedures for aerodynamics on open track, BS EN 14067-4:2005+A1:2009

[2] BSI Eurocode 1 Actions on structures – Part 2 Traffic loads on bridges BS EN 1991-2; 2003

[3] ERRI Loading due to dynamic pressure and suction from railway traffic. Effect of the slipstreams of passing trains on structures adjacent to the track. ERRI D189/RP1, 1994

[4] TSI, Interoperability of the trans-European high speed rail system. Infrastructure sub-system. Directive 96/48/EC 2008/217/E, 2008

[5] TSI, Interoperability of the trans-European high speed rail system. Rolling stock sub-system. Directive 96/48/EC 2008/232/E, 2008

[6] Baker C J, Gilbert T, Jordan S, Sterling M, Quinn A (2011) RSSB PROJECT T750, Review Of Euronorm Design Requirements For Trackside And Overhead Structures Subjected To Transient Aerodynamic Loads, Report to RSSB, 2011

[7] Johnson T, Dalley S, 1/25 scale moving model tests for the TRANSAERO Project. In "TRANSAERO- A European Initiative on Transient Aerodynamics for Railway System Optimisation", pp 123-135, Springer-Verlag Berlin, 2002, ISBN 3-540-433136-3, 2002

[8] RSSB, AeroTRAIN Project – database of UK pressure loading data, 2010

[9] Figura G I, Trackside safety tests at Northallerton. British Rail Research Report RR AER 014, 1993

[10] Johnson T, Aerodynamic forces on East Midlands Parkway station platforms, DeltaRail-ES-2009-025 Issue 1, 2009

[11] Sterling M., Baker C.J., Jordan S.C., Johnson T., A study of the slipstreams of high speed passenger trains and freight trains, Proc. Institute of Mechanical Engineers Part F: Journal of Rail and Rapid Transport. 222, 177-19, 2008

[12] Sanz-Andres A, Laveron, Cuerva A, Baker C, Vehicle-induced loads on pedestrian barriers, Journal of Wind Engineering and Industrial Aerodynamics 92,403-426, 2004

Acknowledgements

The experimental programme was undertaken in connection with the RSSB funded research project T750 'Review of Euronorm design requirements for trackside and overhead structures subjected to transient aerodynamic loads', which was sponsored by the railway industry 'Aerodynamics GB Working Group'.

Notation

A Area of train in analysis of [13] (m^2)

C_p Pressure coefficient $p/0.5\rho v^2$

C_F Integrated force coefficient

C_{FMAX} Maximum integrated force coefficient

C_{FMIN} Minimum integrated force coefficient

h Distance from top of rail to overbridge / canopy (m)

H Height of vertical structure in analysis of Sanz-Andres et al (2004) (m)

p Pressure relative to ambient (Pa)

u Longitudinal slipstream velocity (m/s)

v Lateral slipstream velocity (m/s)

w Vertical slipstream velocity (m/s)

V Train / model velocity (m/s)

x Distance along the track (m)

x_{MAX} Distance of maximum pressure peak from pressure zero crossing point (m)

x_{MIN} Distance of minimum pressure peak from pressure zero crossing point (m)

y Lateral distance from centre of track (m)

y' Lateral distance from edge of platform (m)

Y Lateral distance of vertical structures from centre of track (m)

Y' Lateral distance of vertical structures from platform edge (m)

z Vertical distance from the track (m)

z' Vertical distance from top of platform (m)

ρ Density of air (kg/m^3)

Captions for figures

Figure 1 Pressure transients from passing trains (from [1])

Figure 2 The TRAIN Rig

Figure 3 Test train models

Figure 4 Co-ordinate system

Figure 5 Photographs of modelled structures

Figure 6 Effect of multiple runs and data smoothing on pressure coefficient distributions

Figure 7 Hoarding pressure coefficients at 0.25m height at different distances from nearest rail or from platform edge (a – Class 390, trackside; b- Class 390 – platform; c – Class 158, trackside; d- Class 158 – platform; e – Class 66, trackside; f- Class 66 – platform)

Figure 8 Comparison of pressure coefficients caused by different train models on hoardings (a- trackside hoardings, 0.25m from bottom of hoarding, 0.7m from rail; b – platform hoardings 0.25m above bottom of hoarding, 0.2m from platform edge)

Figure 9 Pressure coefficients on overbridge models caused by passage of Class 390 model (a – lateral peak to peak pressure variation on 10m wide overbridges of different heights; b – centreline pressure distributions on 10m wide overbridges of different heights; c – lateral peak to peak variations on 4.5m high overbridges of different widths; d – centreline pressure distributions on 4.5m high overbridges of different widths)

Figure 10 Pressure coefficients on overbridge models caused by passage of Class 158 model (a – lateral peak to peak pressure variation on 10m wide overbridges of different heights; b – centreline pressure distributions on 10m wide overbridges of different heights)

Figure 11 Pressure coefficients on overbridge models caused by passage of Class 66 model (a – lateral peak to peak pressure variation on 10m wide overbridges of different heights; b – centreline pressure distributions on 10m wide overbridges of different heights; c – lateral peak to peak variations on 4.5m high overbridges of different widths; d – centreline pressure distributions on 4.5m high overbridges of different widths)

Figure 12 Comparison of pressure coefficient distributions for 10m wide, 4.5m high overbridges for all train models

Figure 13 Variation of pressure coefficient across 4.0m high canopy with 2.7m back wall (a – Class 390; b – Class 158; c – Class 66)

Figure 14 Variation of pressure coefficient at edge of canopy for different canopy heights and back wall distances (a – Class 390; b – Class 158; c – Class 66)

Figure 15 Effect of back wall distance on pressures close to leading edge of canopy

Figure 16 Variation of pressure coefficient at the canopy edge with different train types for a 4.0m high canopy with a 2.7m back wall.

Figure 17 Comparison of pressure coefficients caused by all train models close to the edge of the trestle platform

Figure 18 Comparison of earlier TRAIN Rig pressure coefficients measurements on the side of a stationary train with current TRAIN Rig hoarding data, (TRAIN Rig measurements given by solid lines) [8]

Figure 19 Comparison of earlier full scale pressure coefficients measurements on the side of a stationary Class 390 with current TRAIN Rig hoarding data, (TRAIN Rig measurements given by solid lines). [8]

Figure 20 Comparison of current TRAIN Rig hoarding data with full scale Northallerton measurements, (TRAIN Rig measurements given by solid lines) [9]

Figure 21 Comparison of current TRAIN Rig data with full scale East Midland Parkway measurements, (TRAIN Rig measurements given by solid lines). [10]

Figure 22. Slipstream velocity traces around the nose of a Velaro S103 high speed train, 2.5m from the track centre line, 0.2m above top of rail [12] - the graph shows the longitudinal, and lateral components of horizontal slipstream velocity normalised by the train speed; distance is measured from an arbitrary point ahead of the train

Figure 23. Plot of equations (5) – load transients from the analysis of [13]

Figure 24 Normalised pressure transients

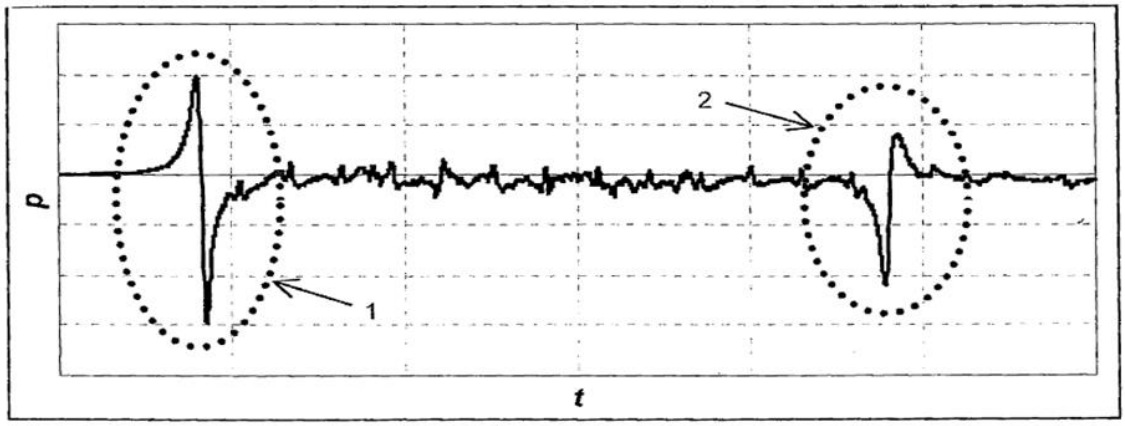

Key

1 Head of train passing

2 Tail of train passing

Figure 1 Pressure transients from passing trains (from [1])

Figure 2 The TRAIN Rig

a) Class 390

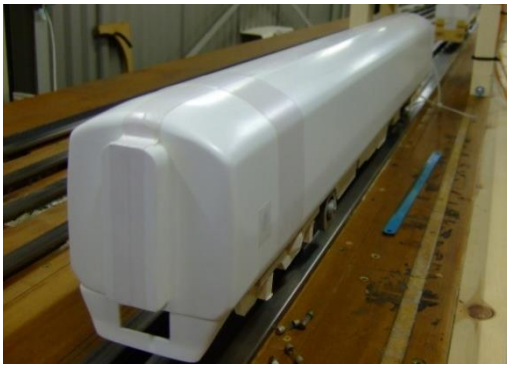

b) Class 158

c) Class 66

Figure 3 Test train models

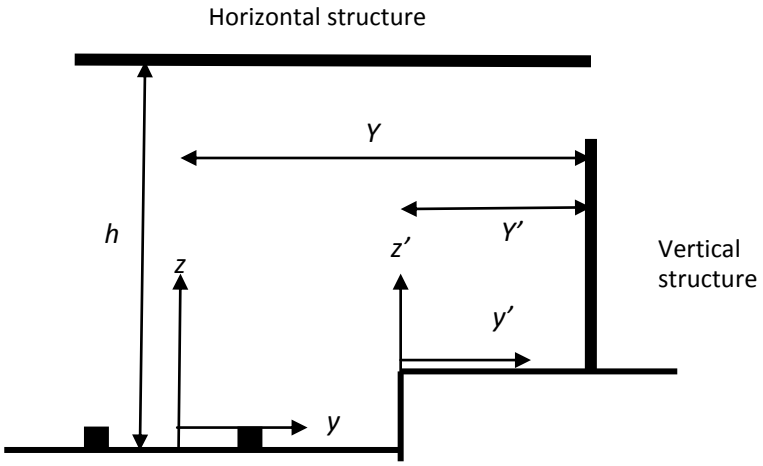

Figure 4 Co-ordinate system

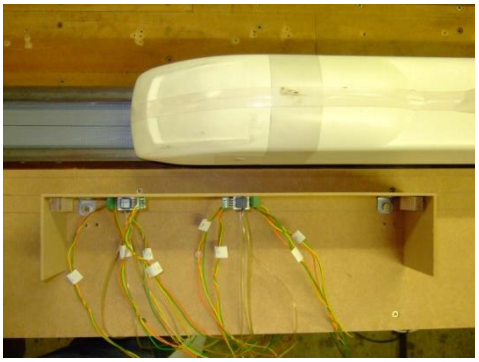

a) Hoarding (from above)

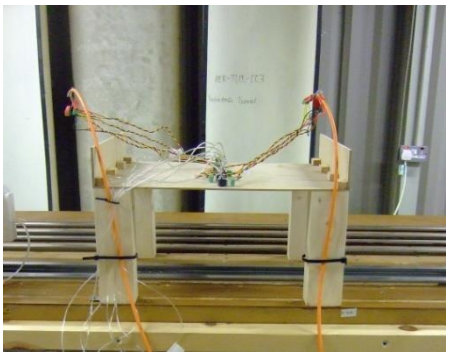

b) Overbridge (from side of track)

c) Canopy

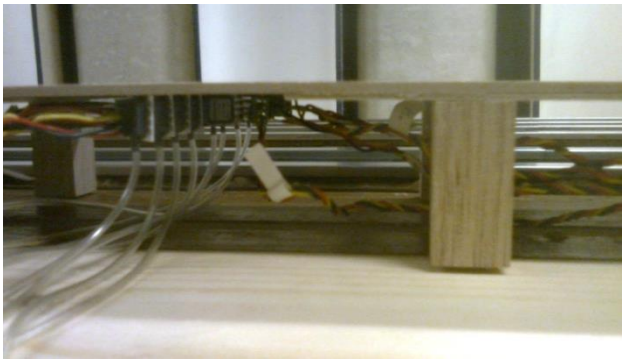

d) Trestle platform (from side of track)

Figure 5 Photographs of modelled structures

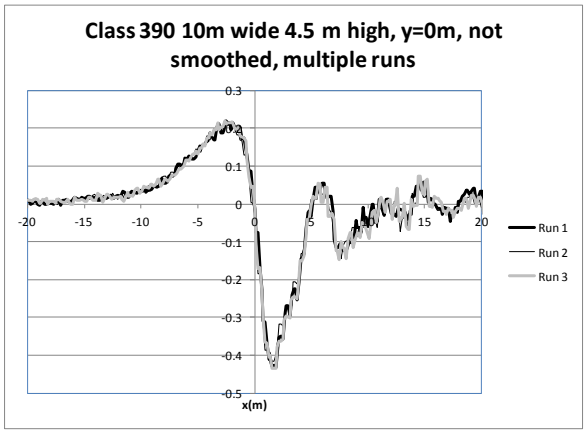

(a)

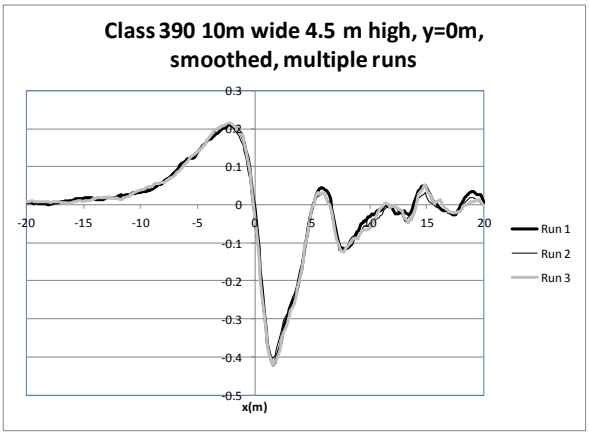

(b)

Figure 6 Effect of multiple runs and data smoothing on pressure coefficient distributions

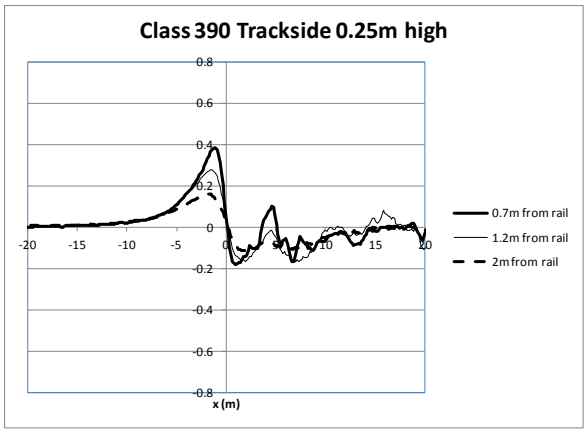

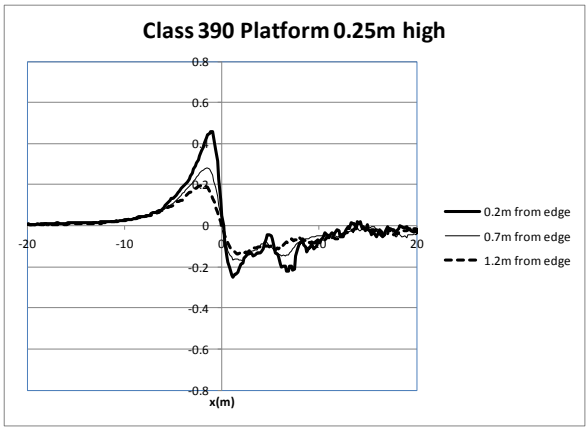

(a) (b)

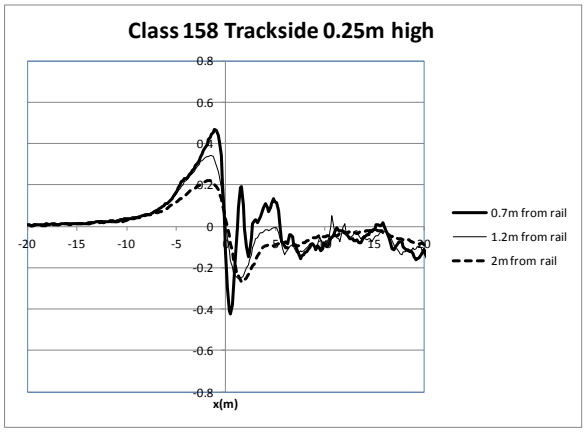

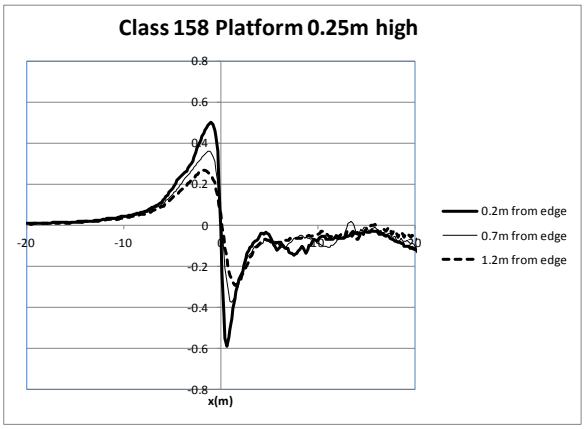

(c) (d)

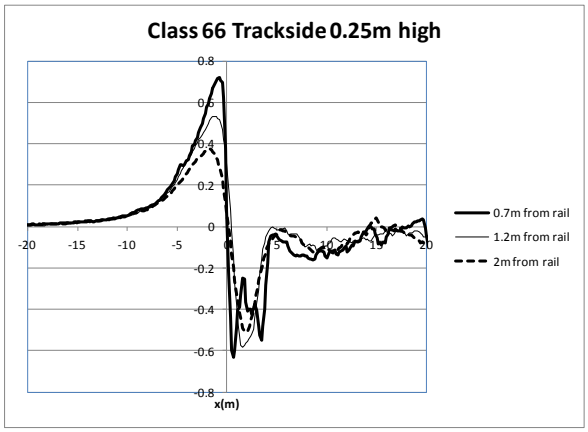

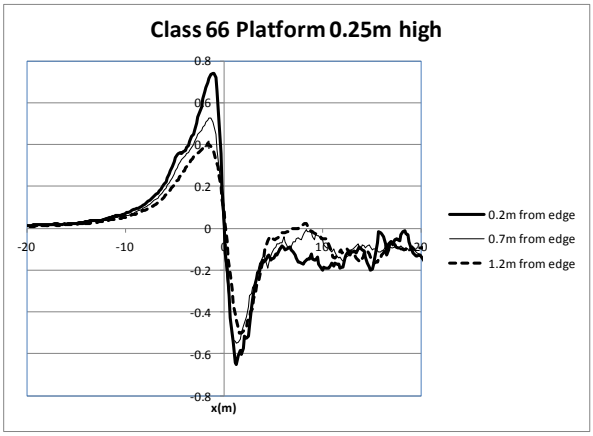

(e) (f)

Figure 7 Hoarding pressure coefficients at 0.25m height at different distances from nearest rail or from platform edge (a – Class 390, trackside; b- Class 390 – platform; c – Class 158, trackside; d- Class 158 – platform; e – Class 66, trackside; f- Class 66 – platform)

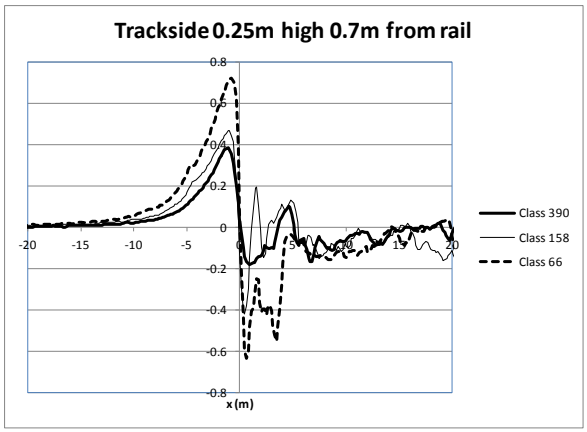

(a)

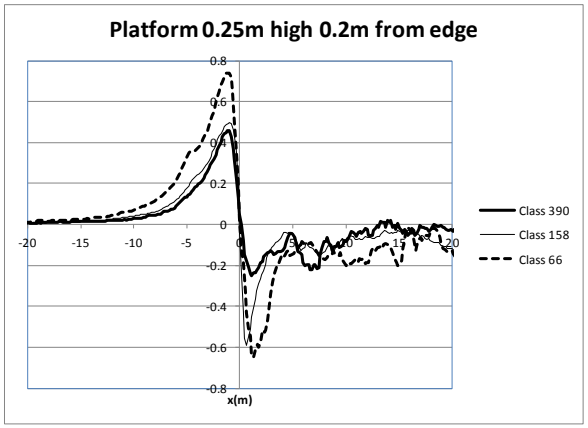

(b)

Figure 8 Comparison of pressure coefficients caused by different train models on hoardings (a- trackside hoardings, 0.25m from bottom of hoarding, 0.7m from rail; b – platform hoardings 0.25m above bottom of hoarding, 0.2m from platform edge)

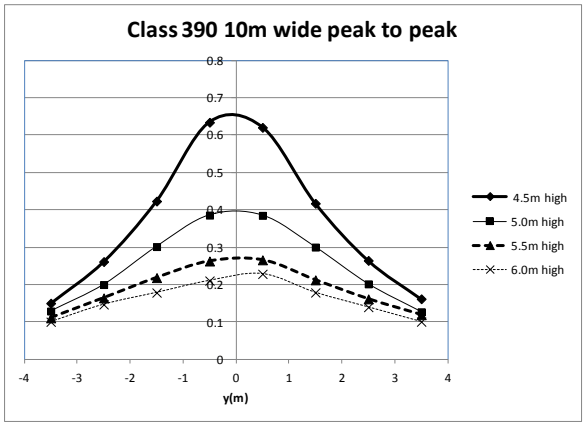

(a)

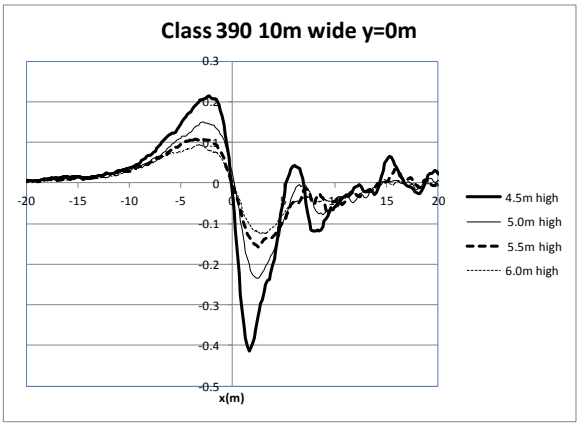

(b)

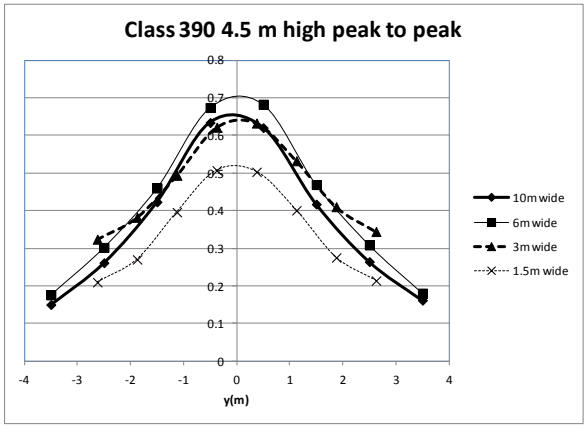

(c)

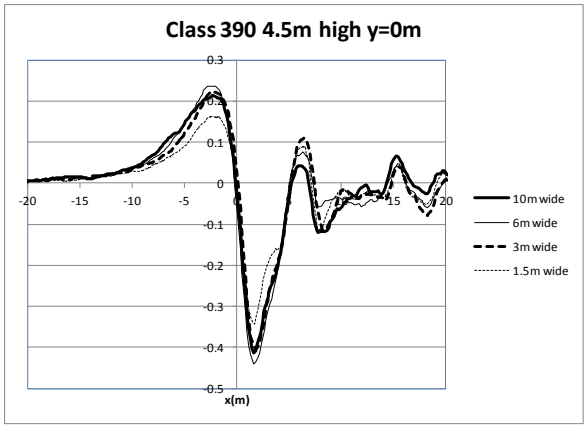

(d)

Figure 9 Pressure coefficients on overbridge models caused by passage of Class 390 model (a – lateral peak to peak pressure variation on 10m wide overbridges of different heights; b – centreline pressure distributions on 10m wide overbridges of different heights; c – lateral peak to peak variations on 4.5m high overbridges of different widths; d – centreline pressure distributions on 4.5m high overbridges of different widths)

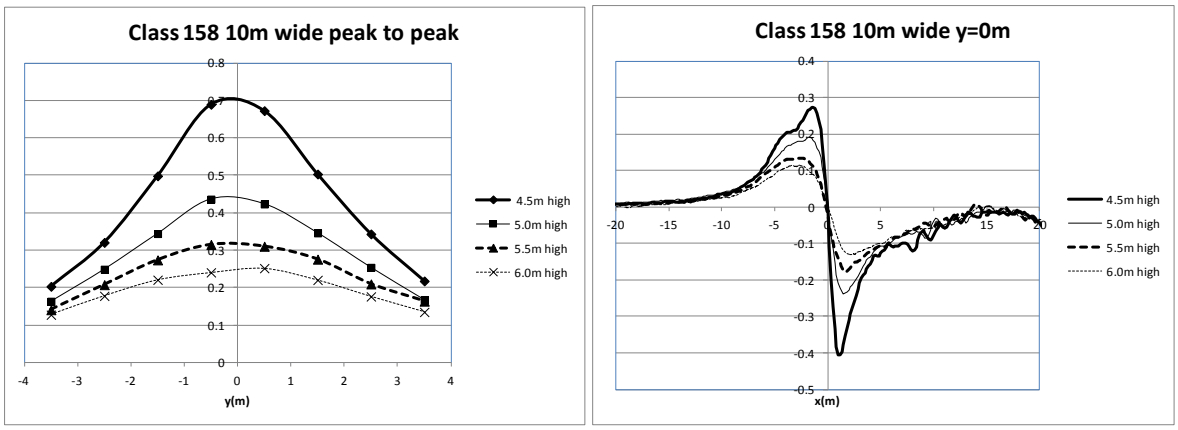

(a) (b)

Figure 10 Pressure coefficients on overbridge models caused by passage of Class 158 model (a – lateral peak to peak pressure variation on 10m wide overbridges of different heights; b – centreline pressure distributions on 10m wide overbridges of different heights)

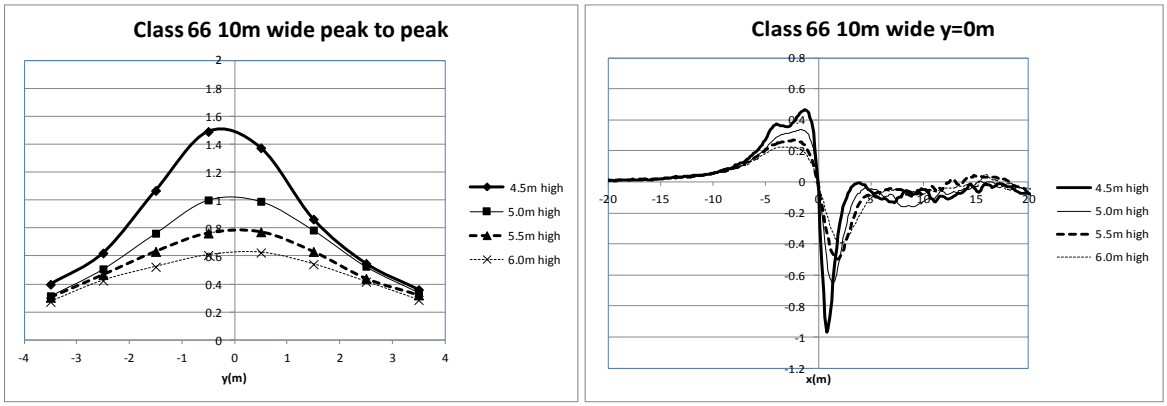

(a) (b)

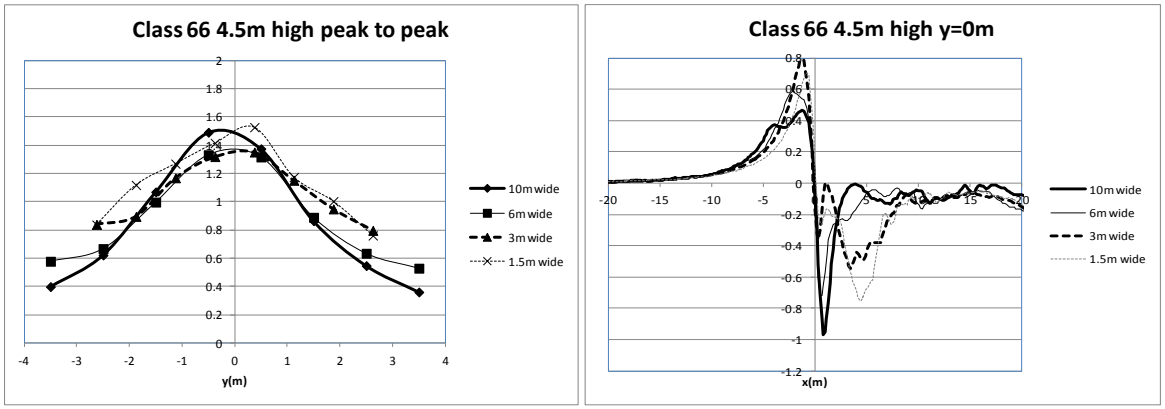

(c) (d)

Figure 11 Pressure coefficients on overbridge models caused by passage of Class 66 model (a – lateral peak to peak pressure variation on 10m wide overbridges of different heights; b – centreline pressure distributions on 10m wide overbridges of different heights; c – lateral peak to peak variations on 4.5m high overbridges of different widths; d – centreline pressure distributions on 4.5m high overbridges of different widths)

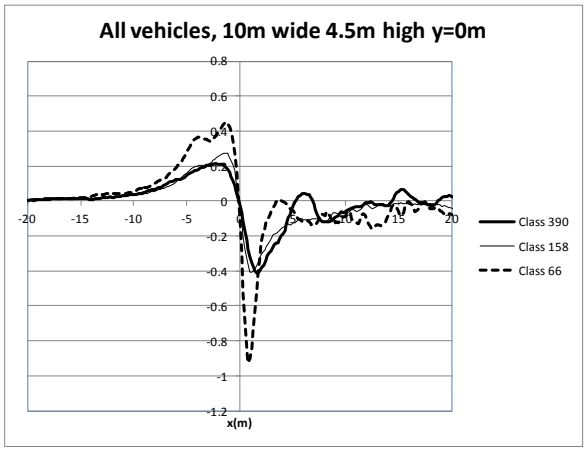

Figure 12 Comparison of pressure coefficient distributions for 10m wide, 4.5m high overbridges for all train models

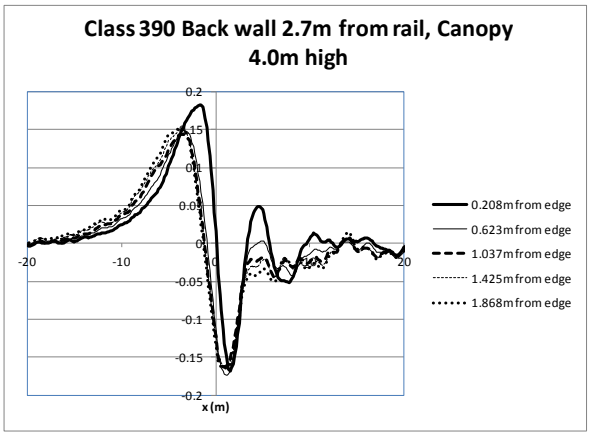

(a)

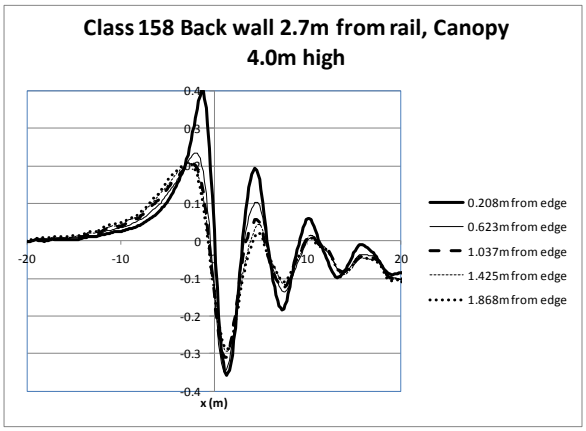

(b)

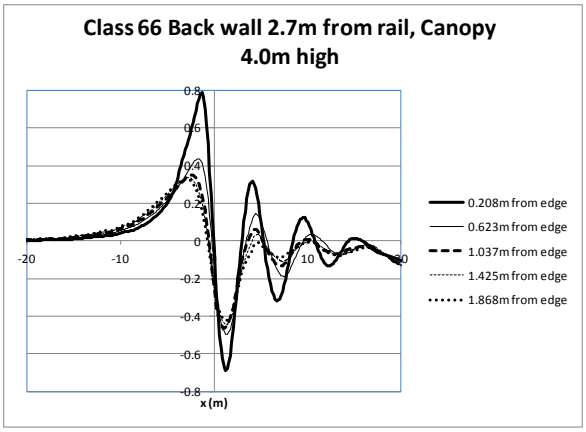

(c)

Figure 13 Variation of pressure coefficient across 4.0m high canopy with 2.7m back wall (a – Class 390; b – Class 158; c – Class 66)

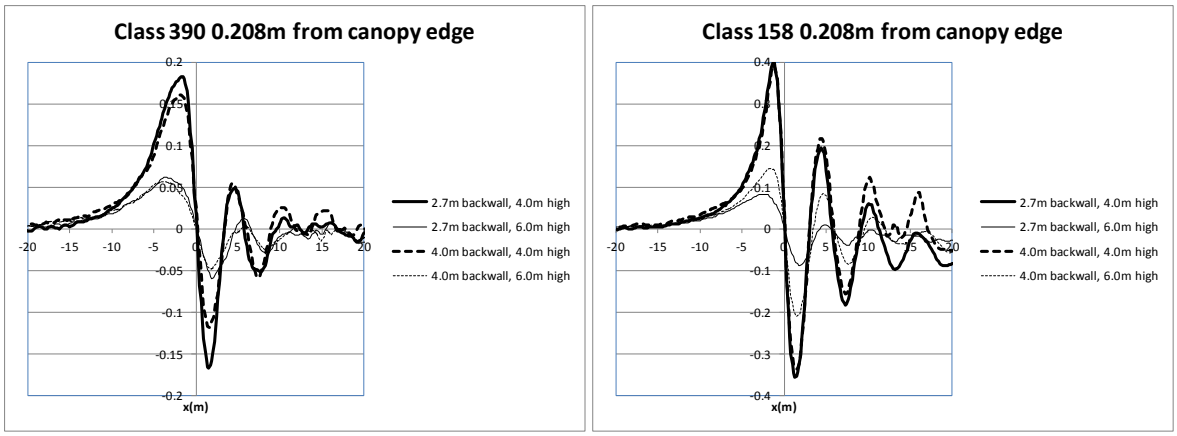

(a) (b)

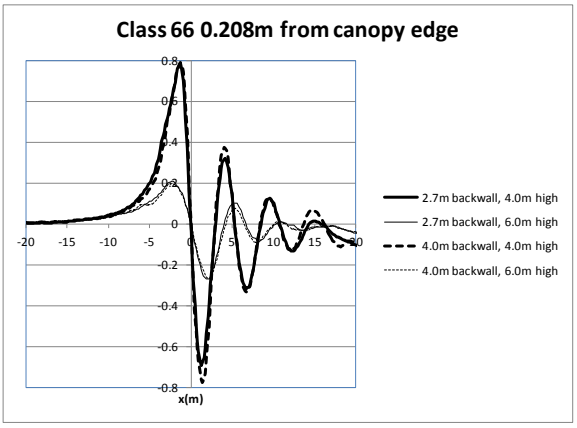

(c)

Figure 14 Variation of pressure coefficient at edge of canopy for different canopy heights and back wall distances (a – Class 390; b – Class 158; c – Class 66)

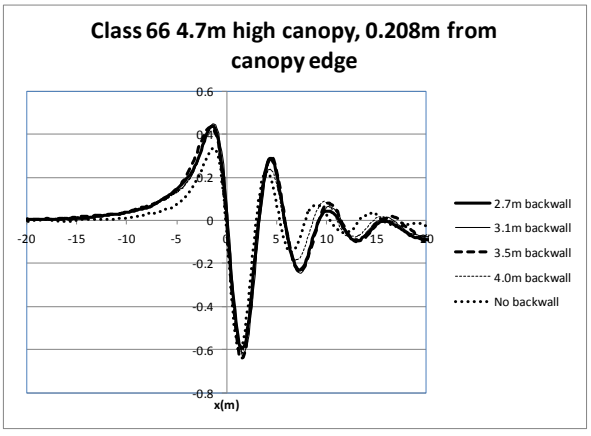

Figure 15 Effect of back wall distance on pressures close to leading edge of canopy

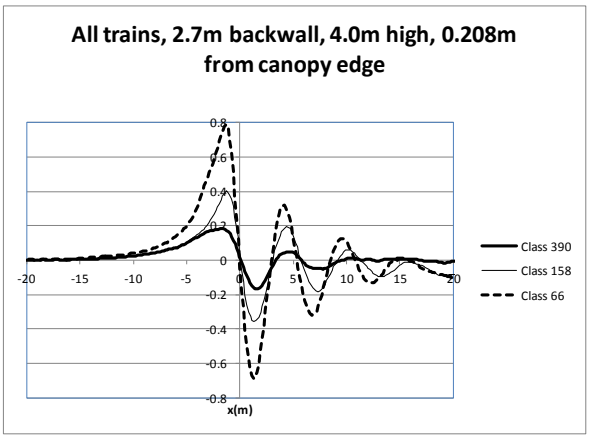

Figure 16 Variation of pressure coefficient at the canopy edge with different train types for a 4.0m high canopy with a 2.7m back wall.

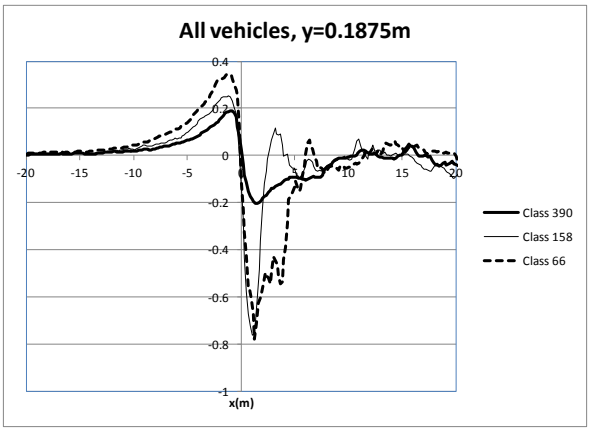

Figure 17 Comparison of pressure coefficients caused by all train models close to the edge of the trestle platform

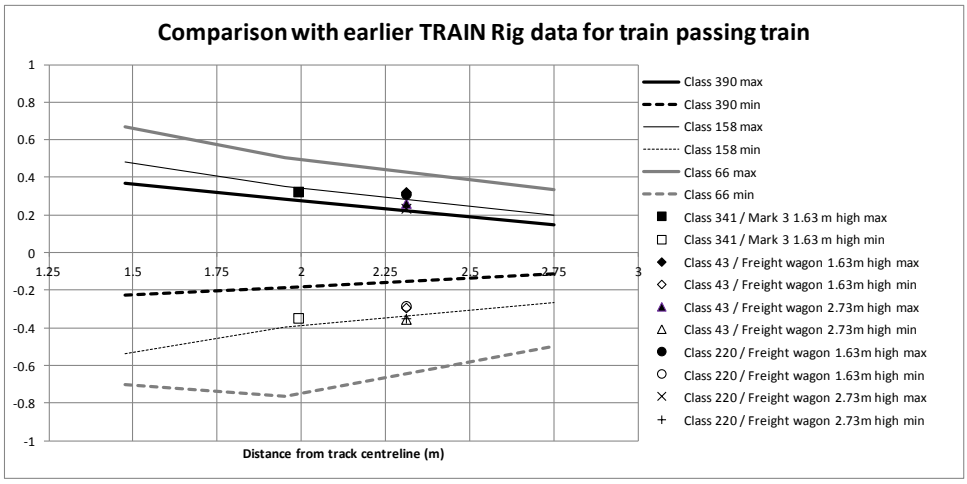

Figure 18 Comparison of earlier TRAIN Rig pressure coefficients measurements on the side of a stationary train with current TRAIN Rig hoarding data, (TRAIN Rig measurements given by solid lines) [8]

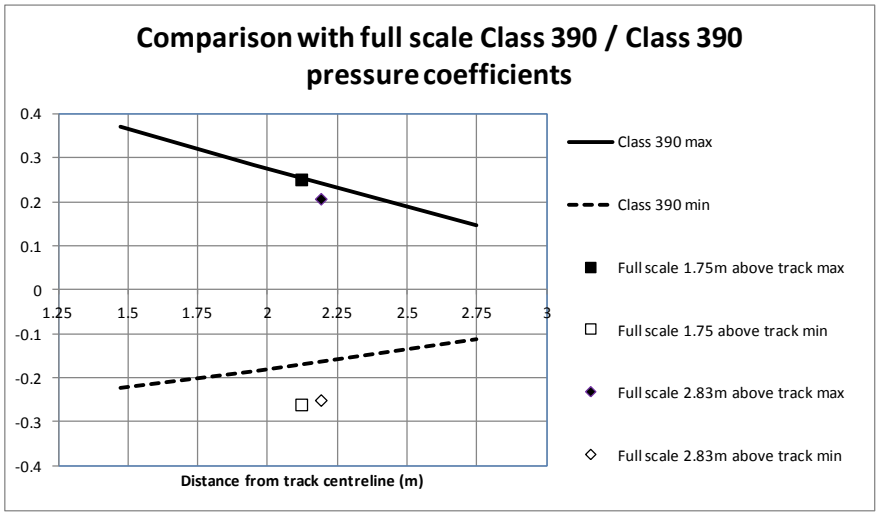

Figure 19 Comparison of earlier full scale pressure coefficients measurements on the side of a stationary Class 390 with current TRAIN Rig hoarding data, (TRAIN Rig measurements given by solid lines). [8]

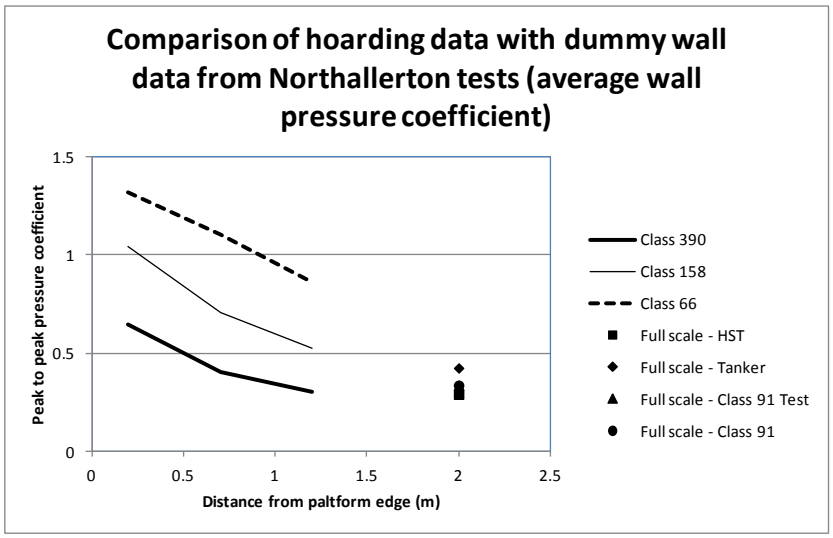

Figure 20 Comparison of current TRAIN Rig hoarding data with full scale Northallerton measurements, (TRAIN Rig measurements given by solid lines) [9]

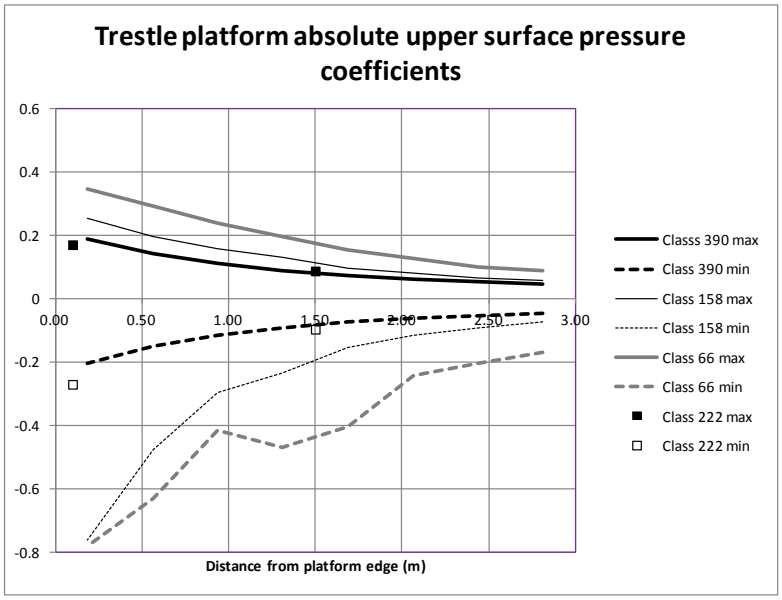

Figure 21 Comparison of current TRAIN Rig data with full scale East Midland Parkway measurements, (TRAIN Rig measurements given by solid lines). [10]

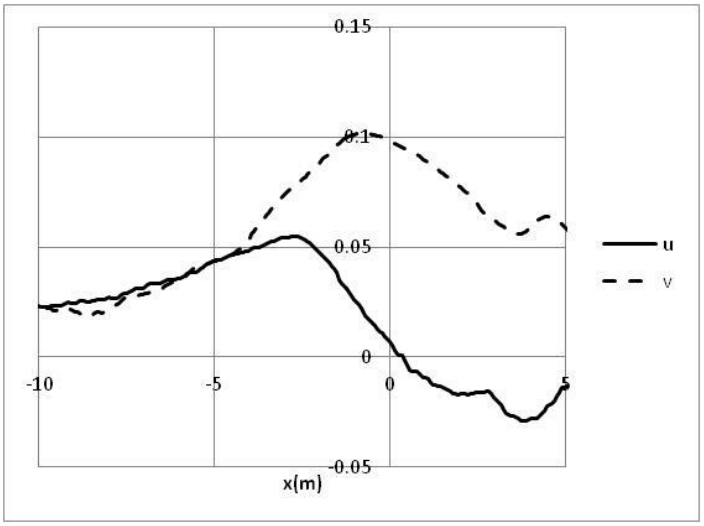

Figure 22. Slipstream velocity traces around the nose of an ICE-1 train, 2.85m from the track centre line, 0.5m above top of rail [11] - the graph shows the longitudinal (u) and lateral (v) components of horizontal slipstream velocity normalised by the train speed; distance is measured from an arbitrary point close to the train nose

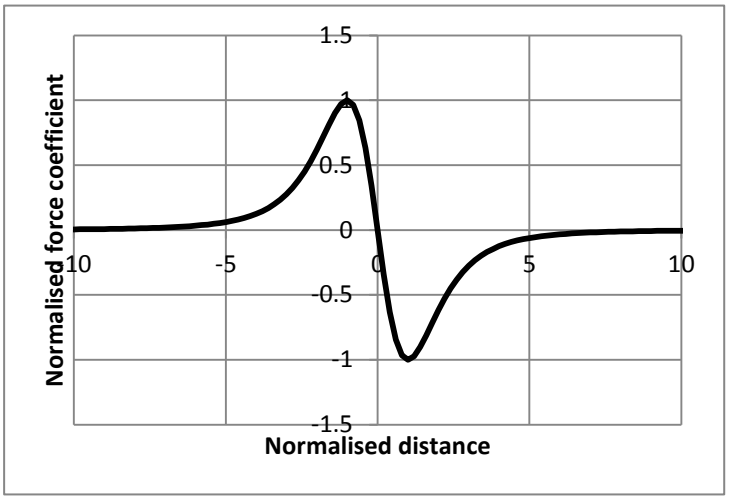

Figure 23. Plot of equations (5) – load transients from the analysis of [12]

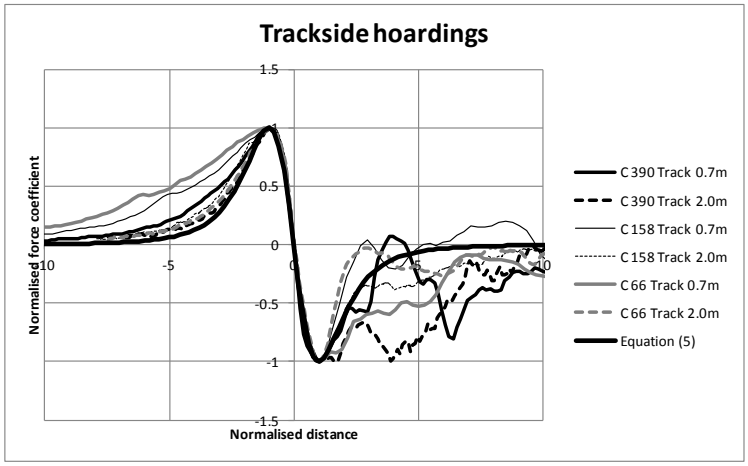

(a) Trackside hoardings

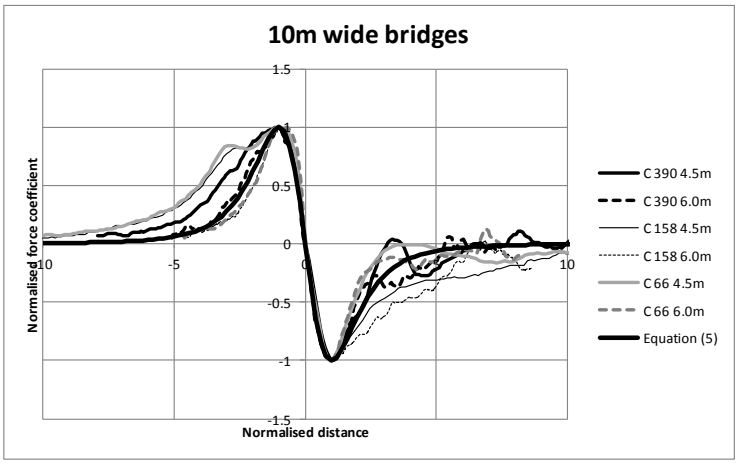

(b) Overbridges

Figure 24 Normalised pressure transients

	Y (m)	C_{Fmax}	C_{Fmin}	x_{max} (m)	x_{min} (m)	C_{Fmax}/C_{Fmin}	x_{max}/x_{min}	C_{Fmax}
Class 390 hoarding	1.45	0.37	-0.21	-1.16	1.06	1.73	1.10	-1.45
	1.95	0.28	-0.18	-1.26	0.96	1.57	1.32	
	2.75	0.15	-0.11	-2.29	1.54	1.35	1.48	
Class 158 hoarding	1.45	0.47	-0.54	-0.86	0.57	0.88	1.51	-1.40
	1.95	0.35	-0.39	-1.33	0.91	0.90	1.46	
	2.75	0.19	-0.27	-2.03	1.47	0.72	1.38	
Class 66 hoarding	1.45	0.67	-0.64	-0.75	0.66	1.05	1.13	-1.09
	1.95	0.52	-0.68	-1.39	1.28	0.76	1.09	
	2.75	0.33	-0.50	-2.16	1.85	0.67	1.17	
Class 390 overbridge	4.50	0.18	-0.34	-2.02	1.89	0.53	1.07	-2.44
	5.00	0.15	-0.24	-3.11	2.26	0.63	1.38	
	5.50	0.11	-0.16	-3.46	2.53	0.68	1.37	
	6.00	0.09	-0.12	-3.31	2.69	0.75	1.23	
Class 158 overbridge	4.50	0.23	-0.35	-1.43	1.25	0.66	1.14	-2.60
	5.00	0.19	-0.24	-1.88	1.46	0.80	1.29	
	5.50	0.13	-0.18	-2.28	1.94	0.75	1.17	
	6.00	0.11	-0.13	-3.47	2.21	0.88	1.57	
Class 66 overbridge	4.50	0.42	-0.84	-1.36	1.00	0.50	1.36	-2.20
	5.00	0.34	-0.66	-1.58	1.41	0.51	1.12	
	5.50	0.27	-0.50	-2.17	1.87	0.54	1.16	
	6.00	0.22	-0.39	-3.49	2.32	0.57	1.50	

Table 1 Scaling parameters of pressure coefficient time history